JACS
JOURNAL OF THE AMERICAN CHEMICAL SOCIETY
pubs.acs.org/JACS
Article

Enantioselective Construction of Quaternary Stereocenters via Cooperative Photoredox/Fe/Chiral Primary Amine Triple Catalysis

Lian-Jie Li, Jun-Chun Zhang, Wei-Peng Li, Dan Zhang, Kaining Duanmu, Hui Yu, Qian Ping, and Ze-Peng Yang*

Cite This: J. Am. Chem. Soc. 2024, 146, 9404–9412
Read Online

ABSTRACT: The catalytic and enantioselective construction of quaternary (all-carbon substituents) stereocenters poses a formidable challenge in organic synthesis due to the hindrance caused by steric factors. One conceptually viable and potentially versatile approach is the coupling of a C−C bond through an outer-sphere mechanism, accompanied by the realization of enantiocontrol through cooperative catalysis; however, examples of such processes are yet to be identified. Herein, we present such a method for creating different compounds with quaternary stereocenters by photoredox/Fe/chiral primary amine triple catalysis. This approach facilitates the connection of an unactivated alkyl source with a tertiary alkyl moiety, which is also rare. The scalable process exhibits mild conditions, does not necessitate the use of a base, and possesses a good functional-group tolerance. Preliminary investigations into the underlying mechanisms have provided valuable insights into the reaction pathway.

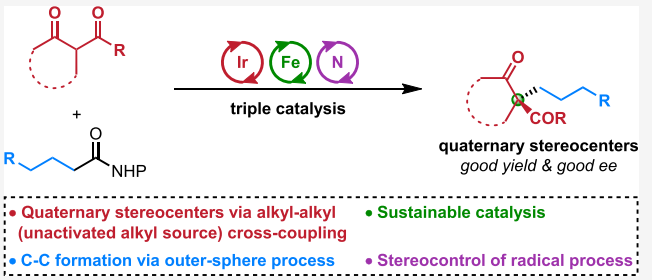

INTRODUCTION

The enantioselective construction of quaternary (all-carbon substituents) stereocenters holds great significance in the realm of organic synthesis, since compounds featuring quaternary stereocenters are prevalent in various applications such as pharmaceuticals, agrochemicals, and other fine chemicals.[1] For example, ∼10% of the top 200 small-molecule pharmaceuticals by retail sales in 2022 contain a quaternary stereocenter.[2] However, the formation of heavily substituted carbon centers presents inherent difficulties owing to the hindrance caused by steric factors. Moreover, achieving enantioselectivity, especially through the utilization of a chiral catalyst rather than relying on substrate control or a stoichiometric chiral reagent, becomes even more challenging when carbon is stereogenic. To this end, various catalytic asymmetric strategies have been developed.[3,4] Among these, the intermolecular enantioselective cross-coupling of a tertiary fragment and a primary fragment emerges as a modular and versatile solution (Figure 1A).[5] Nevertheless, the utilization of a primary unactivated alkyl source in enantioselective alkyl−alkyl cross-coupling remains significantly underexplored. A breakthrough in this field was unveiled in 2018 by the Fu group, who realized an enantioconvergent cross-coupling of a tertiary alkyl electrophile, specifically α-halo-β-lactam, and a primary alkyl nucleophile generated in situ from olefin (Figure 1A, eq 1).[6] Very recently, by implementing a novel bimetallic ligand, the Tao group achieved the α-alkylation of ketones with unactivated alkyl iodides (Figure 1A, eq 2).[7] Notably, both of these examples require basic conditions and are nickel-catalyzed reactions.

Typically, nickel-catalyzed coupling reactions of alkyl species proceed through the involvement of a Ni(III) intermediate, which subsequently undergoes inner-sphere reductive elimination to form C−C bonds (Figure 1B, above).[8−10] Attaching a tertiary alkyl radical to a metal center is a formidable challenge due to the substantial steric hindrance that may arise from such a metal−alkyl intermediate. We speculate that the final C−C formation through an outer-sphere mechanism could potentially offer a viable solution for creating quaternary centers (Figure 1B, below). This approach allows the tertiary alkyl radical to avoid binding to the metal center and instead form a bond at a distant location, at least the length of a metal−carbon bond away from the metal center, thereby reducing potential steric hindrance. In 2022, based on the outer-sphere mechanism, the Liu group presented an elegant Cu-catalyzed enantioconvergent cross-coupling of various tertiary electrophiles with (sp)-hybridized alkynes as the coupling partners.[11]

Iron is the most abundant transition metal in the earth's crust.[12] It is considered to be less toxic in comparison to other

Received: February 5, 2024
Revised: March 7, 2024
Accepted: March 8, 2024
Published: March 20, 2024

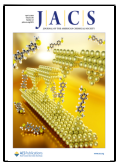

https://doi.org/10.1021/jacs.4c01842
J. Am. Chem. Soc. 2024, 146, 9404−9412

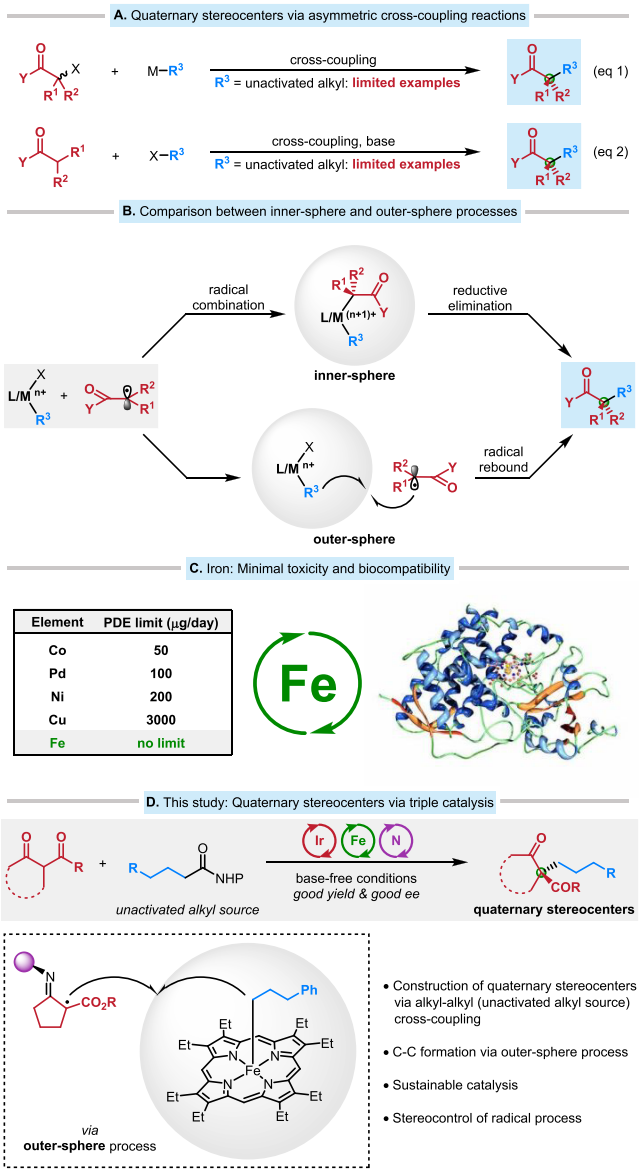

Figure 1. (A) Construction of quaternary stereocenters via catalytic asymmetric cross-coupling reactions. (B) Comparison between cross couplings that occur through inner- and outer-sphere mechanisms. (C) Iron: Minimal toxicity and biocompatibility. (D) This study: Enantioselective construction of quaternary stereocenters via cooperative photoredox/Fe/chiral primary amine triple catalysis.

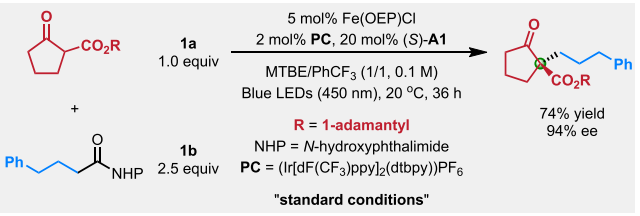

entry	variation from the "**standard conditions**"	yield (%)[a]	ee[b]
1	None	74	94
2	No Fe, **PC**, (*S*)-**A1**, or light	0	–
3	Fe(TPP)Cl, instead of Fe(OEP)Cl	37	78
4	FePc, instead of Fe(OEP)Cl	6	36
5	Fe(III) Protoporphyrin IX, instead of Fe(OEP)Cl	11	74
6	$Ni(acac)_2$+K[Tp*], instead of Fe(OEP)Cl	0	–
7	Vitamin B12, instead of Fe(OEP)Cl	2	–
8	Co(Salen), instead of Fe(OEP)Cl	3	–
9	Co(TPP), instead of Fe(OEP)Cl	0	–
10	**A2**, instead of (*S*)-**A1**	40	87
11	**A3**, instead of (*S*)-**A1**	47	86
12	**A4**, instead of (*S*)-**A1**	35	83
13	**A5**, instead of (*S*)-**A1**	21	88
14	**A6**, instead of (*S*)-**A1**	0	–
15	Pure MTBE	64	94
16	Pure $PhCF_3$	54	94
17	2.5 mol% Fe(OEP)Cl	65	94
18	1.0 mol% **PC**	58	94
19	18 h, instead of 36 h	53	94
20	10 °C, instead of 20 °C	54	95
21	30 °C, instead of 20 °C	60	94
22	0.05 M, instead of 0.1 M	56	95
23	1.0 mL air added	50	94
24	1.0 equiv H_2O added	62	93

[a] Determined through GC analysis. [b] Determined through HPLC analysis.

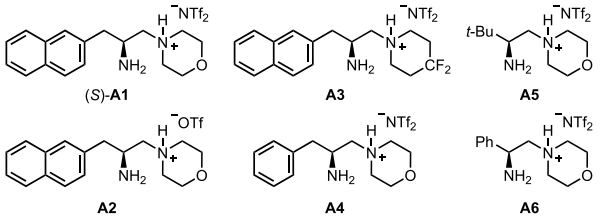

Figure 2. Catalytic enantioselective cross-coupling of a 1,3-dicarbonyl compound and an unactivated alkyl NHP ester.

transition metals and has been an integral component within various biological systems and metabolic processes (Figure 1C).[13] For example, iron is widely present in many metalloenzymes and metalloproteins that are pervasive in both natural environments and the human body. Thus, the application of iron catalysts in chemical reactions is a sustainable approach.[14] The synthesis and characterization of alkyl-Fe (III) porphyrin compounds can be traced back to the 1960s, during which researchers discovered that these complexes could undergo iron−carbon bond homolysis at ambient temperature to generate an alkyl radical.[15] Moreover, due to their open-shell metal complex nature, iron catalysts have been employed in outer-sphere C−C formation reactions.[16] In 2021, the MacMillan group disclosed a pioneering biomimetic S_H2 cross-coupling reaction that allows for the creation of achiral/racemic quaternary carbon centers.[17]

In 2023, the Zhang group's study highlighted the exciting potential of iron(III)-based metalloradical catalysis in advancing asymmetric cyclopropanation reactions (most cases focus on tertiary stereocenters).[18] Very recently, the Shenvi group discovered an iron porphyrin catalyst capable of facilitating iterative outer-sphere steps.[19]

Despite these significant advances, creating quaternary stereocenters asymmetrically via iron-catalyzed outer-sphere alkyl−alkyl cross-coupling, particularly with unactivated alkyl sources, remains a challenge. Drawing upon the seminal work on ternary catalysis by Luo and co-workers,[20,21] we propose a photoredox/Fe/chiral primary amine triple catalysis scheme for a novel approach to generating quaternary stereocenters with enantiocontrol (Figure 5D). Notably, enantioselective organocatalysis was recognized as one of the ten emerging technologies in chemistry with the potential to make our planet more sustainable by IUPAC on its 100th anniversary in 2019.[22] In this report, we describe the realization of this objective, specifically, that the combination of iron and chiral primary amine catalysts can achieve the sustainable coupling of 1,3-dicarbonyl compounds with unactivated alkyl NHP (*N*-hydroxyphthalimide) esters under base-free conditions, providing ready access to a wide variety of quaternary stereocenters (Figure 1D).

https://doi.org/10.1021/jacs.4c01842
J. Am. Chem. Soc. 2024, 146, 9404−9412

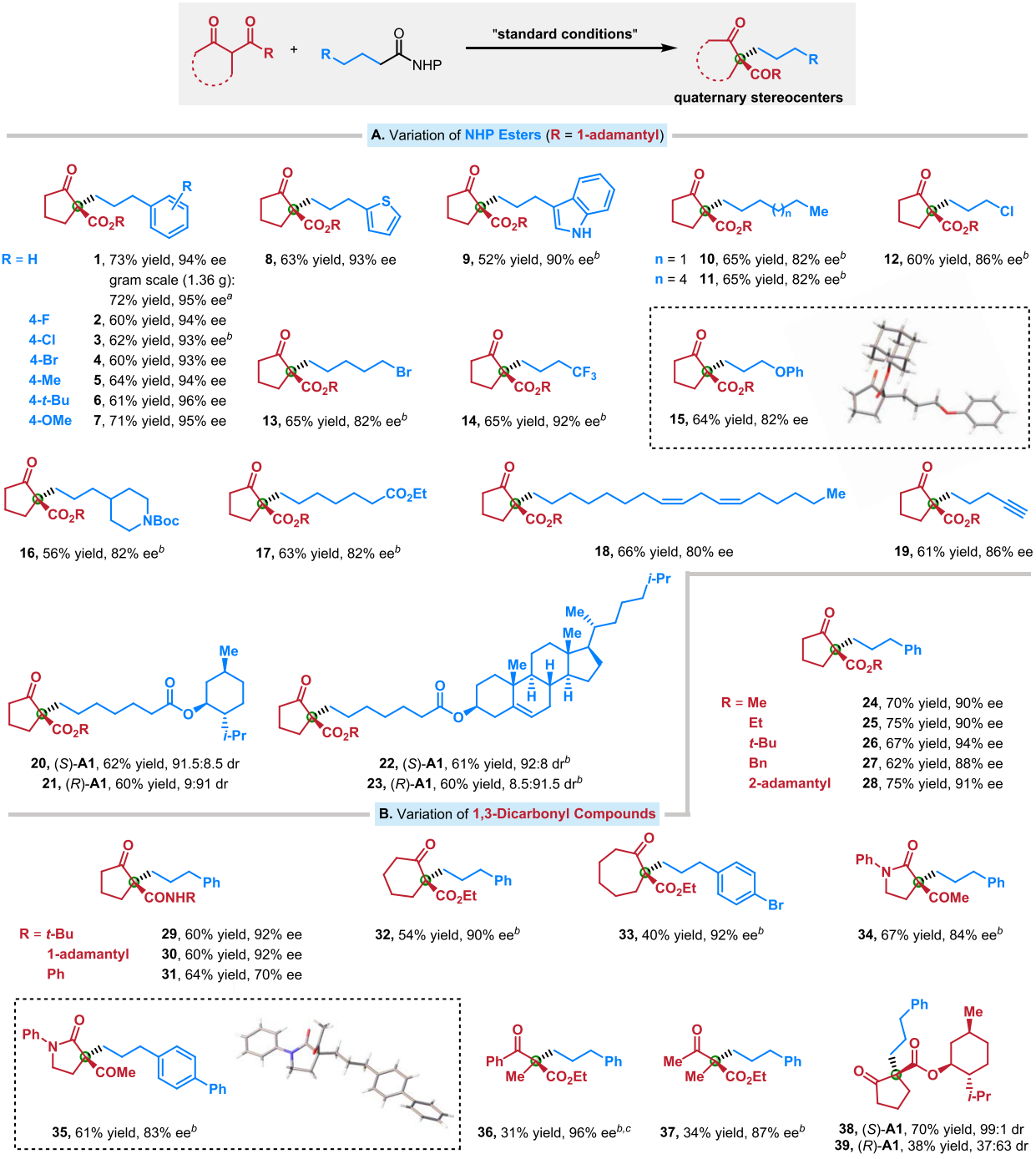

[a] 96 h, instead of 36 h. [b] 72 h, instead of 36 h. [c] $(Ir[dFppy]_2(bpy))PF_6$, instead of $(Ir[dF(CF_3)ppy]_2(dtbpy))PF_6$.

Figure 3. Scope of catalytic enantioselective cross-coupling. All couplings were conducted on a 0.20 mmol scale (unless otherwise noted), and all yields are of purified products.

RESULTS AND DISCUSSION

Reaction Optimization. In an initial study, we examined the coupling of 1-adamantyl 2-oxocyclopentane carboxylate **1a** with an unactivated alkyl NHP ester **1b** (Figure 2). After an extensive evaluation of all reaction parameters, we determined that Fe(OEP)Cl (III, OEP = 2,3,7,8,12,13,17,18-octaethyl-21*H*,23*H*-porphine) and chiral primary amine (*S*)-**A1** can accomplish the desired enantioselective cross-coupling in good yield and ee (74% yield, 92% ee; entry 1). It is worth noting that no additional base was required for the enolization of **1a**, therefore rendering this method a mild way to establish quaternary stereocenters.

In the absence of Fe(OEP)Cl, photocatalyst (**PC**), (*S*)-**A1**, or light, essentially no product is observed (entry 2).[23] Employing other iron catalysts, such as Fe(TPP)Cl (III, TPP = 5,10,15,20-tetraphenyl-21*H*,23*H*-porphyrin), FePc (II, iron phthalocyanine), or Fe(III) protoporphyrin IX, resulted in a product with much lower efficiency and selectivity (entries 3−5). Other catalysts capable of facilitating bimolecular homolytic substitution, such as $Ni(acac)_2$ (II, acac =

https://doi.org/10.1021/jacs.4c01842
J. Am. Chem. Soc. 2024, 146, 9404−9412

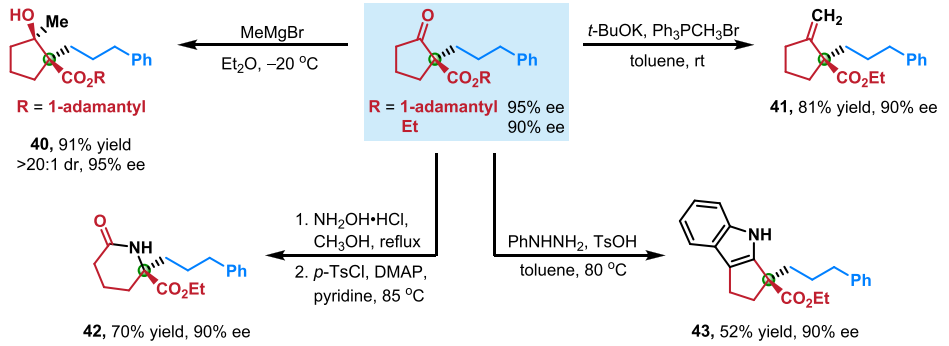

Figure 4. Transformations into other useful families of enantioenriched compounds.

acetylacetonate) and K[Tp*] (potassium tri(3,5-dimethyl-1-pyrazolyl)borohydride), Vitamin B12, Co(Salen) (II, Salen = *N*,*N*′-bis(salicylidene)ethylenediamine), or Co(TPP) (II), yielded negligible or no product (entries 6−9). A variety of other chiral primary amines are less effective than (*S*)-**A1** (entries 10−14).[24] Moreover, the mixed solvent proved superior to a single solvent (entries 15 and 16). If the coupling process is carried out with a lower amount of iron or photocatalyst, for a shorter duration, at a lower temperature (10 °C) or a higher temperature (30 °C), or in a solution that is diluted, then the yield obtained will be lower while still maintaining almost the same ee (entries 17−22). Notably, the reaction proceeds relatively smoothly in the presence of a small amount of air or water (entries 23 and 24).

Substrate Scope. With the optimized reaction conditions in hand, we sought to examine the generality of the substrate scope for both coupling partners. This straightforward method for the catalytic enantioselective synthesis of quaternary stereocenters is compatible with an array of unactivated alkyl NHP esters (Figure 3A), providing a range of products with good yields and high ee. For example, many aryls prove to be appropriate, including heteroaryls, such as thiophene and indole (products **1**−**9**). A variety of functional groups can be present, including unactivated primary alkyl chloride/bromide, trifluoromethyl, ether, Boc-protected amine, ester, internal olefin, and terminal alkyne (products **10**−**19**). Several products on the list have the potential to serve as intermediates in the preparation of bioactive compounds. One such example is product **11**, which is a derivative of a well-established precursor of (+)-Malyngolide, an antibiotic that exhibits significant activity against *Mycobacterium smegmatis* and *Streptococcus pyogenes*.[25] Product **19**, on the other hand, could potentially be used to synthesize Ptaquilosin, a compound that has shown antitumor activity and toxicity toward myelocytic leukemia.[26] In the case of an NHP ester that bears stereocenters at a remote position, the stereochemistry of the amine catalyst, rather than that of the NHP ester, controls the stereochemistry of the coupling product (products **20**−**23**). On a gram scale (1.36 g of product), the coupling to generate product **1** proceeds in almost identical yield and ee as for a reaction conducted on a 0.20 mmol scale.

We next evaluated the scope of 1,3-dicarbonyl compounds (Figure 3B). This protocol can efficiently incorporate 2-oxocyclopentane carboxylates containing alkyl substituents that vary in size from methyl to 2-adamantyl to *tert*-butyl, and consistently good yields and ee values are observed (products **1**, **24**−**28**). Furthermore, 2-oxocyclopentane carboxamides prove to be appropriate, although a reduction in enantiomeric excess was observed with the *N*-phenyl substrate (products **29**−**31**). To our delight, 1,3-dicarbonyl compounds possessing six- or seven-membered ring structures successfully deliver the corresponding coupling products with good enantioselectivity (products **32** and **33**). We also investigated the coupling of 3-acetyl-1-phenylpyrrolidin-2-one and found it could readily participate under optimal conditions, affording the products with satisfactory results (products **34** and **35**). Not only cyclic compounds but also acyclic ones illustrate superior selectivity, albeit with moderate efficiencies (products **36** and **37**). In the case of a 1,3-dicarbonyl compound that bears stereocenters, employment of (*S*)-**A1** displays excellent diastereoselectivity, while a low diastereoselectivity was obtained for **39**, possibly due to the chirality mismatch between the chiral substrate and (*R*)-**A1**. The absolute configuration of the products was unambiguously determined through X-ray diffraction analysis of compounds **15** and **35**.

Applications and Mechanistic Observations. To showcase the synthetic utility of this new method, we converted the resulting products into a range of other valuable enantioenriched compounds (Figure 4). For example, the carbonyl group of the coupling products could be converted directly in good yields, without racemization, into tertiary alcohol, olefin, δ-lactam, and indole (products **40**−**43**).

To gain further insight into the triple catalysis system, a series of mechanistic studies were conducted. When a coupling is performed in the presence of TEMPO (2,2,6,6-tetramethyl-1-piperidinyloxy), adducts derived from both **1a** and **1b** are isolated, consistent with the generation of organic radicals from each reaction partner (Figure 5A).

The photoinduced electron transfer (PET) process can occur in two distinct ways: (i) reductive quenching, whereby the photocatalyst accepts an electron from a reductant, or (ii) oxidative quenching, whereby the photocatalyst donates an electron to an oxidant. In order to clarify the true pathway, cyclic voltammetry (CV) experiments and analyses were carried out (Figure 5B.**1**). The enamine species **E** was synthesized and its potential, as well as that of **1b**, were measured (half-wave potential $E_{1/2}$ ($\mathbf{E}^{+\cdot}/\mathbf{E}$) = +1.03 V vs saturated calomel electrode (SCE) in MeCN; $E_{1/2}$ ($\mathbf{1b}/\mathbf{1b}^{-\cdot}$) = −1.17 V vs SCE in MeCN). The potentials of the photocatalyst are known (for reductive quenching: $E_{1/2}$ ($\mathbf{PC}^*/\mathbf{PC}^-$) = +1.21 V vs SCE in MeCN; $E_{1/2}$ ($\mathbf{PC}/\mathbf{PC}^-$) = −1.37 V vs SCE in MeCN; for oxidative quenching: $E_{1/2}$ ($\mathbf{PC}^+/\mathbf{PC}^*$) = −0.89 V vs SCE in MeCN; $E_{1/2}$ ($\mathbf{PC}^+/\mathbf{PC}$) = +1.69 V vs SCE in MeCN).[27] While both $\mathbf{PC}^*$ and $\mathbf{PC}^+$ can oxidize **E**, only $\mathbf{PC}^-$ can reduce **1b**, whereas **PC*** can hardly do so (−0.89 V vs −1.17 V).[28,29] Therefore, it can be concluded

https://doi.org/10.1021/jacs.4c01842
J. Am. Chem. Soc. 2024, 146, 9404−9412

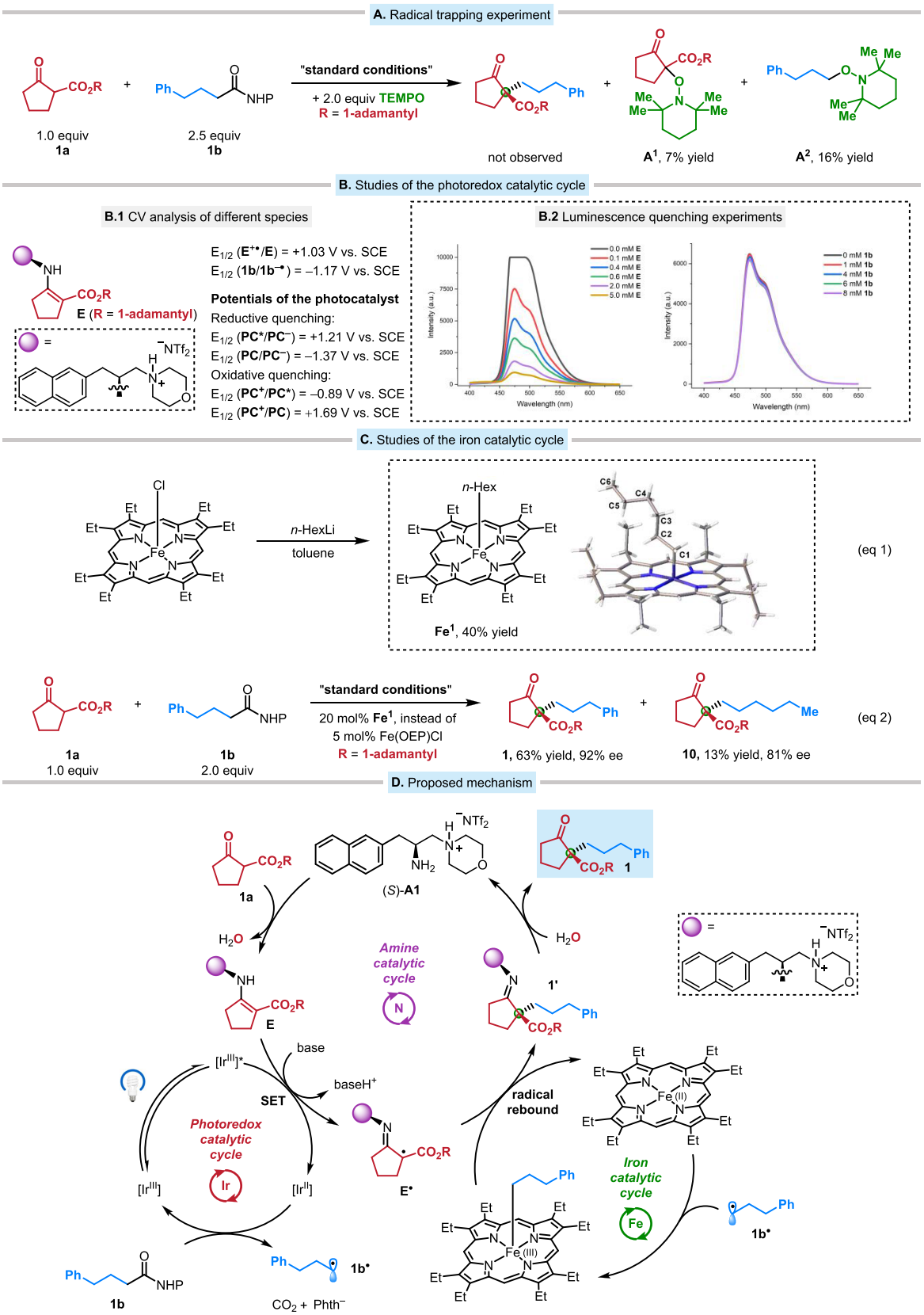

Figure 5. (A) Radical trapping experiment using TEMPO. (B) Mechanistic studies of the photoredox catalytic cycle. (C) Mechanistic studies of the iron catalytic cycle. (D) Plot of a plausible mechanism.

that the PET proceeds through a reductive quenching mechanism, which is further supported by Stern–Volmer studies. The excited state of **PC** has a relatively long lifetime (2.3 μs), and the Stern–Volmer studies demonstrated that the luminescence of the excited state of **PC** is readily quenched by

https://doi.org/10.1021/jacs.4c01842
J. Am. Chem. Soc. 2024, 146, 9404–9412

enamine **E**, whereas NHP ester **1b** was not found to be an effective quencher (Figure 5B.2).

With regard to the iron catalytic cycle, we propose that Fe(OEP) (II) generated in situ can capture an unhindered primary alkyl radical to form an alkyl-Fe(OEP) (III) species, which in turn undergoes an outer-sphere radical rebound with the tertiary alkyl radical to produce a coupling intermediate.[17a] To validate this hypothesis, we prepared a potential catalytic intermediate, an alkyl-Fe(OEP) (III) species **Fe^1**, by adding *n*-hexyl lithium to a solution of Fe(OEP)Cl (Figure 5C, eq 1). **Fe^1** was characterized by ^{1}HNMR, HRMS, and X-ray diffraction, which revealed a five-coordinate Fe (III) complex with porphine in the equatorial plane and *n*-hexyl as the axial ligand. The Fe−C1 bond has a bond length of 2.027(5) Å, which closely resembles the bond length of Fe−C in the alkyl-Fe(TPP) species (2.030(2) Å).[15c] Interestingly, the C1−C2 bond length (1.489(8) Å) is shorter compared to the other C−C bonds within the hexyl group, suggesting that C1 exhibits a portion of (sp^2)-hybridization. Moreover, Due to the absence of an open position cis to the carbon ligand on iron, C−C formation by inner-sphere reductive elimination becomes impossible. We further examined the utilization of 20 mol % of **Fe^1** as both a catalytic intermediate and a precatalyst in the cross-coupling between **1a** and **1b** (Figure 5C, eq 2). To our delight, desired product **1** was obtained with 63% yield and 92% ee, which is similar to the outcome obtained when Fe(OEP)Cl was employed. Notably, the incorporation of the *n*-hexyl moiety into the coupling product (**10**) provides direct evidence of the involvement of the alkyl-Fe(OEP) (III) species in the cross-coupling reaction.

Based on the above findings and prior studies, a plausible mechanism for the model reaction is proposed in Figure 5D. The reaction commences with condensation of the chiral primary amine catalyst (*S*)-**A1** and 1,3-dicarbonyl compound **1a**, yielding enamine **E**. Concurrently, irradiation of the iridium photocatalyst [Ir^{III}] with blue light-emitting diodes (LEDs) generates the long-lived excited-state complex [Ir^{III}]*. This highly oxidizing charge transfer species is capable of facilitating single-electron transfer (SET) from the electron-rich enamine **E**, resulting in the production of reduced [Ir^{II}] and a critical enaminyl radical species **E**$^{\cdot}$. Next, [Ir^{II}] reduces NHP ester **1b** to give the primary alkyl radical **1b**$^{\cdot}$, which is captured by Fe(OEP) (II), leading to the formation of alkyl-Fe(OEP) (III). After that, an outer-sphere radical rebound takes place between **E**$^{\cdot}$ and alkyl-Fe(OEP) (III), resulting in the establishment of the C−C bond, while alkyl-Fe(OEP) (III) reverts back to Fe(OEP) (II). Finally, hydrolysis of **1'** yields the coupling product.

CONCLUSIONS

We have developed a new method for creating different compounds with quaternary stereocenters through photoredox/Fe/chiral primary amine triple catalysis. The approach is modular and sustainable, and it allows for the coupling of an unactivated alkyl source via an outer-sphere C−C formation mechanism with good enantiocontrol. This scalable process is mild and base-free and has good functional-group tolerance. Several coupling products could serve as potential intermediates for the preparation of bioactive compounds and can be transformed into other valuable compounds. Preliminary mechanistic studies, including radical trapping, CV analysis, Stern−Volmer quenching, catalytic intermediate isolation, and a control experiment, have shed light on the reaction pathway. Given the importance of quaternary stereocenters and broad interest in metallaphotoredox catalysis, we believe that this protocol will encourage further exploration of cooperative catalytic systems to unlock a plethora of previously challenging asymmetric transformations. Additional efforts to apply earth-abundant metals to useful asymmetric coupling reactions are underway in our laboratory.

ASSOCIATED CONTENT

Supporting Information

The Supporting Information is available free of charge at https://pubs.acs.org/doi/10.1021/jacs.4c01842.

Experimental details: general information, preparation of chiral primary amines, preparation of 1,3-dicarbonyl compounds and NHP esters, catalytic enantioselective cross-couplings, effect of reaction parameters, unsuccessful examples, applications, mechanistic experiments, assignments of absolute configuration, and NMR spectra and determination of stereoselectivity (PDF)

Accession Codes

CCDC 2330035, 2307691, 2314298 contain the supplementary crystallographic data for this paper. These data can be obtained free of charge via www.ccdc.cam.ac.uk/data_request/cif, or by emailing data_request@ccdc.cam.ac.uk, or by contacting The Cambridge Crystallographic Data Centre, 12 Union Road, Cambridge CB2 1EZ, UK; fax: + 44 1223 336033.

AUTHOR INFORMATION

Corresponding Author

Ze-Peng Yang − *Shanghai Key Laboratory of Chemical Assessment and Sustainability, School of Chemical Science and Engineering, Tongji University, Shanghai 200092, People's Republic of China;* orcid.org/0000-0003-0248-1963; Email: zpyang@tongji.edu.cn

Authors

Lian-Jie Li − *Shanghai Key Laboratory of Chemical Assessment and Sustainability, School of Chemical Science and Engineering, Tongji University, Shanghai 200092, People's Republic of China;* orcid.org/0009-0006-9552-1408

Jun-Chun Zhang − *Shanghai Key Laboratory of Chemical Assessment and Sustainability, School of Chemical Science and Engineering, Tongji University, Shanghai 200092, People's Republic of China;* orcid.org/0009-0000-2754-8322

Wei-Peng Li − *Shanghai Key Laboratory of Chemical Assessment and Sustainability, School of Chemical Science and Engineering, Tongji University, Shanghai 200092, People's Republic of China;* orcid.org/0009-0005-6596-9781

Dan Zhang − *Shanghai Key Laboratory of Chemical Assessment and Sustainability, School of Chemical Science and Engineering, Tongji University, Shanghai 200092, People's Republic of China;* orcid.org/0009-0002-1490-6826

Kaining Duanmu − *Shanghai Key Laboratory of Chemical Assessment and Sustainability, School of Chemical Science and Engineering, Tongji University, Shanghai 200092, People's Republic of China;* orcid.org/0000-0002-9865-8710

Hui Yu − *Shanghai Key Laboratory of Chemical Assessment and Sustainability, School of Chemical Science and Engineering, Tongji University, Shanghai 200092, People's Republic of China;* orcid.org/0000-0002-5717-6635

Qian Ping − *State Key Laboratory of Pollution Control and Resource Reuse, College of Environmental Science and Engineering, Tongji University, Shanghai 200092, People's Republic of China;* orcid.org/0000-0001-6707-8361

Complete contact information is available at: https://pubs.acs.org/10.1021/jacs.4c01842

Notes

The authors declare no competing financial interest.

■ ACKNOWLEDGMENTS

We thank Prof. Weijun Kong (Tongji University) for helpful suggestions and discussions on CV studies. Support has been provided by the National Natural Science Foundation of China (Grant No. 22201216), the National Key Research & Development Program of China (Grant No. 2023YFA1508600), and the Fundamental Research Funds for the Central Universities (Grant No. 22120230252, 2023-3-YB-10).

■ REFERENCES

(1) (a) Peterson, E. A.; Overman, L. E. Contiguous stereogenic quaternary carbons: A daunting challenge in natural products synthesis. *Proc. Natl. Acad. Sci. U. S. A.* **2004**, *101*, 11943−11948. (b) Ling, T.; Rivas, F. All-carbon quaternary centers in natural products and medicinal chemistry: recent advances. *Tetrahedron* **2016**, *72*, 6729−6777. (c) Li, C.; Ragab, S. S.; Liu, G.; Tang, W. Enantioselective formation of quaternary carbon stereocenters in natural product synthesis: a recent update. *Nat. Prod. Rep.* **2020**, *37*, 276−292. (d) Talele, T. T. Opportunities for Tapping into Three-Dimensional Chemical Space through a Quaternary Carbon. *J. Med. Chem.* **2020**, *63*, 13291−13315.

(2) *Top 200 Posters*. https://sites.arizona.edu/njardarson-lab/top200-posters/ (accessed 2024−02−01).

(3) For selected reviews, see: (a) Quasdorf, K. W.; Overman, L. E. Catalytic enantioselective synthesis of quaternary carbon stereocentres. *Nature* **2014**, *516*, 181−191. (b) Liu, Y.; Han, S.-J.; Liu, W.-B.; Stoltz, B. M. Catalytic Enantioselective Construction of Quaternary Stereocenters: Assembly of Key Building Blocks for the Synthesis of Biologically Active Molecules. *Acc. Chem. Res.* **2015**, *48*, 740−751. (c) Zeng, X.-P.; Cao, Z.-Y.; Wang, Y.-H.; Zhou, F.; Zhou, J. Catalytic Enantioselective Desymmetrization Reactions to All-Carbon Quaternary Stereocenters. *Chem. Rev.* **2016**, *116*, 7330−7396. (d) Feng, J.; Holmes, M.; Krische, M. J. Acyclic Quaternary Carbon Stereocenters via Enantioselective Transition Metal Catalysis. *Chem. Rev.* **2017**, *117*, 12564−12580. (e) Süsse, L.; Stoltz, B. M. Enantioselective Formation of Quaternary Centers by Allylic Alkylation with First-Row Transition-Metal Catalysts. *Chem. Rev.* **2021**, *121*, 4084−4099.

(4) For selected recent examples, see: (a) Krautwald, S.; Sarlah, D.; Schafroth, M. A.; Carreira, E. M. Enantio- and Diastereodivergent Dual Catalysis: α-Allylation of Branched Aldehydes. *Science* **2013**, *340*, 1065−1068. (b) Mei, T.-S.; Patel, H. H.; Sigman, M. S. Enantioselective construction of remote quaternary stereocentres. *Nature* **2014**, *508*, 340−344. (c) Zhu, Y.; Zhang, L.; Luo, S. Asymmetric α-Photoalkylation of β-Ketocarbonyls by Primary Amine Catalysis: Facile Access to Acyclic All-Carbon Quaternary Stereocenters. *J. Am. Chem. Soc.* **2014**, *136*, 14642−14645. (d) Kita, Y.; Kavthe, R. D.; Oda, H.; Mashima, K. Asymmetric Allylic Alkylation of β-Ketoesters with Allylic Alcohols by a Nickel/Diphosphine Catalyst. *Angew. Chem., Int. Ed.* **2016**, *55*, 1098−1101. (e) Wendlandt, A. E.; Vangal, P.; Jacobsen, E. N. Quaternary stereocentres via an enantioconvergent catalytic S_N1 reaction. *Nature* **2018**, *556*, 447−451. (f) Hervieu, C.; Kirillova, M. S.; Suárez, T.; Müller, M.; Merino, E.; Nevado, C. Asymmetric, visible light-mediated radical sulfinyl-Smiles rearrangement to access all-carbon quaternary stereocentres. *Nat. Chem.* **2021**, *13*, 327−334. (g) Chen, Z.-H.; Sun, R.-Z.; Yao, F.; Hu, X.-D.; Xiang, L.-X.; Cong, H.; Liu, W.-B. Enantioselective Nickel-Catalyzed Reductive Aryl/Alkenyl−Cyano Cyclization Coupling to All-Carbon Quaternary Stereocenters. *J. Am. Chem. Soc.* **2022**, *144*, 4776−4782. (h) Ghosh, S.; Erchinger, J. E.; Maji, R.; List, B. Catalytic Asymmetric Spirocyclizing Diels-Alder Reactions of Enones: Stereoselective Total and Formal Syntheses of α-Chamigrene, β-Chamigrene, Laurencenone C, Colletoic Acid, and Omphalic Acid. *J. Am. Chem. Soc.* **2022**, *144*, 6703−6708. (i) Wang, K.; Yang, L.; Li, Y.; Li, H.; Liu, Z.; Ning, L.; Liu, X.; Feng, X. Asymmetric Catalytic Ring-Expansion of 3-Methyleneazetidines with α-Diazo Pyrazoamides towards Proline-Derivatives. *Angew. Chem., Int. Ed.* **2023**, *62*, No. e202307249. (j) Wen, Y.-H.; Yang, F.; Li, S.; Yao, X.; Song, J.; Gong, L.-Z. Diastereodivergent Desymmetric Annulation to Access Spirooxindoles: Chemical Probes for Mitosis. *J. Am. Chem. Soc.* **2023**, *145*, 4199−4207. (k) Yu, Z.-L.; Cheng, Y.-F.; Liu, J.-R.; Yang, W.; Xu, D.-T.; Tian, Y.; Bian, J.-Q.; Li, Z.-L.; Fan, L.-W.; Luan, C.; Gao, A.; Gu, Q.-S.; Liu, X.-Y. Cu(I)-Catalyzed Chemo- and Enantioselective Desymmetrizing C-O Bond Coupling of Acyl Radicals. *J. Am. Chem. Soc.* **2023**, *145*, 6535−6545. (l) Song, J.; Zheng, W.-H. Synthesis of a C_2-Symmetric Chiral Borinic Acid and Its Application in Catalytic Desymmetrization of 2,2-Disubstituted-1,3-Propanediols. *J. Am. Chem. Soc.* **2023**, *145*, 8338−8343. (m) Shen, J.; Xu, Z.; Yang, S.; Li, S.; Jiang, J.; Zhang, Y.-Q. Quaternary Stereocenters via Catalytic Enantioconvergent Allylation of Epoxides. *J. Am. Chem. Soc.* **2023**, *145*, 21122−21131. (n) Pan, G.; Pu, M.; Wang, H.; Ying, M.; Li, Y.; Dong, S.; Feng, X.; Liu, X. Catalytic Enantioselective Nucleophilic Addition to Arynes by a New Quaternary Guanidinium Salt-Based Phase-Transfer Catalyst. *J. Am. Chem. Soc.* **2023**, *145*, 26318−26327. (o) Peng, L.; Wang, M.; Huang, J.; Guo, C.; Gong, L.-Z.; Song, J. Enantio- and Diastereodivergent N-Heterocyclic Carbene/Nickel Dual-Catalyzed Umpolung Propargylic Substitutions of Enals. *J. Am. Chem. Soc.* **2023**, *145*, 28085−28085. (p) Kadarauch, M.; Whalley, D. M.; Phipps, R. J. sSPhos: A General Ligand for Enantioselective Arylative Phenol Dearomatization via Electrostatically-Directed Palladium Catalysis. *J. Am. Chem. Soc.* **2023**, *145*, 25553−25558. (q) Wakchaure, V. N.; DeSnoo, W.; Laconsay, C. J.; Leutzsch, M.; Tsuji, N.; Tantillo, D. J.; List, B. Catalytic asymmetric cationic shifts of aliphatic hydrocarbons. *Nature* **2024**, *625*, 287−292. (r) Zhang, J.; Zhu, W.; Chen, Z.; Zhang, Q.; Guo, C. Dual-Catalyzed Stereodivergent Electrooxidative Homocoupling of Benzoxazolyl Acetate. *J. Am. Chem. Soc.* **2024**, *146*, 1522−1531.

(5) (a) Wang, Z.; Yang, Z.-P.; Fu, G. C. Quaternary stereocentres via catalytic enantioconvergent nucleophilic substitution reactions of tertiary alkyl halides. *Nat. Chem.* **2021**, *13*, 236−242. (b) Wang, F.-L.; Liu, L.; Yang, C.-J.; Luan, C.; Yang, J.; Chen, J.-J.; Gu, Q.-S.; Li, Z.-L.; Liu, X.-Y. Synthesis of α-Quaternary β-Lactams via Copper-Catalyzed Enantioconvergent Radical $C(sp^3)-C(sp^2)$ Cross-Coupling with Organoboronate Esters. *Angew. Chem., Int. Ed.* **2023**, *62*, No. e202214709.

(6) Wang, Z.; Yin, H.; Fu, G. C. Catalytic enantioconvergent coupling of secondary and tertiary electrophiles with olefins. *Nature* **2018**, *563*, 379−383.

(7) Wang, P.; Zhu, L.; Wang, J.; Tao, Z. Catalytic Asymmetric α-Alkylation of Ketones with Unactivated Alkyl Halides. *J. Am. Chem. Soc.* **2023**, *145*, 27211−27217.

(8) For selected reviews, see: (a) Cherney, A. H.; Kadunce, N. T.; Reisman, S. E. Enantioselective and Enantiospecific Transition-Metal-Catalyzed Cross-Coupling Reactions of Organometallic Reagents To Construct C−C Bonds. *Chem. Rev.* **2015**, *115*, 9587−9652. (b) Iwasaki, T.; Kambe, N. Ni-Catalyzed C−C Couplings Using Alkyl Electrophiles. *Top. Curr. Chem.* **2016**, *374*, 66. (c) Fu, G. C. Transition-Metal Catalysis of Nucleophilic Substitution Reactions: A Radical Alternative to S_N1 and S_N2 Processes. *ACS Cent. Sci.* **2017**, *3*, 692−700. (d) Choi, J.; Fu, G. C. Transition metal−catalyzed alkyl-

alkyl bond formation: Another dimension in cross-coupling chemistry. *Science* **2017**, *356*, No. eaaf7230. (e) Kaga, A.; Chiba, S. Engaging Radicals in Transition Metal-Catalyzed Cross-Coupling with Alkyl Electrophiles: Recent Advances. *ACS Catal.* **2017**, *7*, 4697−4706.

(9) For selected mechanistic studies, see: (a) Schley, N. D.; Fu, G. C. Nickel-Catalyzed Negishi Arylations of Propargylic Bromides: A Mechanistic Investigation. *J. Am. Chem. Soc.* **2014**, *136*, 16588−16593. (b) Yin, H.; Fu, G. C. Mechanistic Investigation of Enantioconvergent Kumada Reactions of Racemic α-Bromoketones Catalyzed by a Nickel/Bis(oxazoline) Complex. *J. Am. Chem. Soc.* **2019**, *141*, 15433−15440. (c) Dawson, G. A.; Spielvogel, E. H.; Diao, T. Nickel-Catalyzed Radical Mechanisms: Informing Cross-Coupling for Synthesizing Non-Canonical Biomolecules. *Acc. Chem. Res.* **2023**, *56*, 3640−3653.

(10) For selected examples that go through outer-sphere mechanism, see: (a) Bour, J. R.; Ferguson, D. M.; McClain, E. J.; Kampf, J. W.; Sanford, M. S. Connecting Organometallic Ni(III) and Ni(IV): Reactions of Carbon-Centered Radicals with High-Valent Organonickel Complexes. *J. Am. Chem. Soc.* **2019**, *141*, 8914−8920. (b) Yuan, M.; Song, Z.; Badir, S. O.; Molander, G. A.; Gutierrez, O. On the Nature of C(sp^3)-C(sp^2) Bond Formation in Nickel-Catalyzed Tertiary Radical Cross-Couplings: A Case Study of Ni/Photoredox Catalytic Cross-Coupling of Alkyl Radicals and Aryl Halides. *J. Am. Chem. Soc.* **2020**, *142*, 7225−7234. (c) Dong, Z.; MacMillan, D. W. C. Metallaphotoredox-enabled deoxygenative arylation of alcohols. *Nature* **2021**, *598*, 451−456. (d) Tsymbal, A. V.; Bizzini, L. D.; MacMillan, D. W. C. Nickel Catalysis via S_H2 Homolytic Substitution: The Double Decarboxylative Cross-Coupling of Aliphatic Acids. *J. Am. Chem. Soc.* **2022**, *144*, 21278−21286. (e) Mao, E.; MacMillan, D. W. C. Late-Stage C(sp^3)-H Methylation of Drug Molecules. *J. Am. Chem. Soc.* **2023**, *145*, 2787−2793.

(11) Wang, F.-L.; Yang, C.-J.; Liu, J.-R.; Yang, N.-Y.; Dong, X.-Y.; Jiang, R.-Q.; Chang, X.-Y.; Li, Z.-L.; Xu, G.-X.; Yuan, D.-L.; Zhang, Y.-S.; Gu, Q.-S.; Hong, X.; Liu, X.-Y. Mechanism-based ligand design for copper-catalysed enantioconvergent C(sp^3)−C(sp) cross-coupling of tertiary electrophiles with alkynes. *Nat. Chem.* **2022**, *14*, 949−957.

(12) Morgan, J. W.; Anders, E. Chemical composition of Earth, Venus, and Mercury. *Proc. Natl. Acad. Sci. U. S. A.* **1980**, *77*, 6973−6977.

(13) (a) Frey, P. A.; Reed, G. H. The Ubiquity of Iron. *ACS Chem. Biol.* **2012**, *7*, 1477−1481. (b) *Guideline for elemental impurities*. https://database.ich.org/sites/default/files/Q3D-R2_Guideline_Step4_2022_0308.pdf (accessed 2024−02−01).

(14) For selected reviews, see: (a) Bauer, I.; Knölker, H.-J. Iron Catalysis in Organic Synthesis. *Chem. Rev.* **2015**, *115*, 3170−3387. (b) Rana, S.; Biswas, J. P.; Paul, S.; Paik, A.; Maiti, D. Organic synthesis with the most abundant transition metal−iron: from rust to multitasking catalysts. *Chem. Soc. Rev.* **2021**, *50*, 243−472. For a book, see: (c) Plietker, B. *Iron Catalysis in Organic Chemistry*; Wiley-VCH: Weinheim, 2008.

(15) For selected examples on the synthesis of alkyl-Fe (III) porphyrin compounds, see: (a) Clarke, D. A.; Dolphin, D.; Grigg, R.; Johnson, A. W.; Pinnock, H. A. Alkyl-, Aryl-, and Acyl-metal(iii) Complexes of Aetioporphyrin I. *J. Chem. Soc. C* **1968**, 881−885. (b) Lexa, D.; Mispelter, J.; Savéant, J.-M. Electroreductive Alkylation of Iron in Porphyrin Complexes. Electrochemical and Spectral Characteristics of α-Alkyliron Porphyrins. *J. Am. Chem. Soc.* **1981**, *103*, 6806−6812. (c) Oh, Y.; Swenson, D.; Goff, H. M. Olefin Polymerization Activity and Crystal Structure of Alkyliron(III) Porphyrin Complexes. *Bull. Korean Chem. Soc.* **2003**, *24*, 167−172. For selected examples on the synthesis of other alkyl-Fe (III) compounds, see: (d) Bouwkamp, M. W.; Lobkovsky, E.; Chirik, P. J. Bis(imino)pyridine Iron(II) Alkyl Cations for Olefin Polymerization. *J. Am. Chem. Soc.* **2005**, *127*, 9660−9661. (e) Tondreau, A. M.; Milsmann, C.; Patrick, A. D.; Hoyt, H. M.; Lobkovsky, E.; Wieghardt, K.; Chirik, P. J. Synthesis and Electronic Structure of Cationic, Neutral, and Anionic Bis(imino)pyridine Iron Alkyl Complexes: Evaluation of Redox Activity in Single-Component Ethylene Polymerization Catalysts. *J. Am. Chem. Soc.* **2010**, *132*, 15046−15059.

(16) For selected iron-catalyzed reactions that may go through inner-sphere mechanism, see: (a) Jin, M.; Adak, L.; Nakamura, M. Iron-Catalyzed Enantioselective Cross-Coupling Reactions of α-Chloroesters with Aryl Grignard Reagents. *J. Am. Chem. Soc.* **2015**, *137*, 7128−7134. (b) Adak, L.; Kawamura, S.; Toma, G.; Takenaka, T.; Isozaki, K.; Takaya, H.; Orita, A.; Li, H. C.; Shing, T. K. M.; Nakamura, M. Synthesis of Aryl *C*-Glycosides via Iron-Catalyzed Cross Coupling of Halosugars: Stereoselective Anomeric Arylation of Glycosyl Radicals. *J. Am. Chem. Soc.* **2017**, *139*, 10693−10701. (c) Sharma, A. K.; Sameera, W. M. C.; Jin, M.; Adak, L.; Okuzono, C.; Iwamoto, T.; Kato, M.; Nakamura, M.; Morokuma, K. DFT and AFIR Study on the Mechanism and the Origin of Enantioselectivity in Iron-Catalyzed Cross-Coupling Reactions. *J. Am. Chem. Soc.* **2017**, *139*, 16117−16125. (d) Liu, L.; Aguilera, M. C.; Lee, W.; Youshaw, C. R.; Neidig, M. L.; Gutierrez, O. General method for iron-catalyzed multicomponent radical cascades−cross-couplings. *Science* **2021**, *374*, 432−439.

(17) (a) Liu, W.; Lavagnino, M. N.; Gould, C. A.; Alcázar, J.; MacMillan, D. W. C. A biomimetic S_H2 cross-coupling mechanism for quaternary sp^3-carbon formation. *Science* **2021**, *374*, 1258−1263. (b) Gould, C. A.; Pace, A. L.; MacMillan, D. W. C. Rapid and Modular Access to Quaternary Carbons from Tertiary Alcohols via Bimolecular Homolytic Substitution. *J. Am. Chem. Soc.* **2023**, *145*, 16330−16336.

(18) Lee, W.-C. C.; Wang, D.-S.; Zhu, Y.; Zhang, X. P. Iron(III)-based metalloradical catalysis for asymmetric cyclopropanation via a stepwise radical mechanism. *Nat. Chem.* **2023**, *15*, 1569−1580.

(19) (a) Gan, X.-C.; Kotesova, S.; Castanedo, A.; Green, S. A.; Møller, S. L. B.; Shenvi, R. A. Iron-Catalyzed Hydrobenzylation: Stereoselective Synthesis of (−)-Eugenial C. *J. Am. Chem. Soc.* **2023**, *145*, 15714−15720. (b) Kong, L.; Gan, X.-C.; van der Puyl Lovett, V. A.; Shenvi, R. A. Alkene Hydrobenzylation by a Single Catalyst That Mediates Iterative Outer-Sphere Steps. *J. Am. Chem. Soc.* **2024**, *146*, 2351−2357.

(20) Jia, Z.; Zhang, L.; Luo, S. Asymmetric C-H Dehydrogenative Allylic Alkylation by Ternary Photoredox-Cobalt-Chiral Primary Amine Catalysis under Visible Light. *J. Am. Chem. Soc.* **2022**, *144*, 10705−10710.

(21) (a) Zhou, H.; Zhang, L.; Xu, C.; Luo, S. Chiral Primary Amine/Palladium Dual Catalysis for Asymmetric Allylic Alkylation of β-Ketocarbonyl Compounds with Allylic Alcohols. *Angew. Chem., Int. Ed.* **2015**, *54*, 12645−12648. (b) Zhou, H.; Wang, Y.; Zhang, L.; Cai, M.; Luo, S. Enantioselective Terminal Addition to Allenes by Dual Chiral Primary Amine/Palladium Catalysis. *J. Am. Chem. Soc.* **2017**, *139*, 3631−3634. (c) Wang, Y.; Chai, J.; You, C.; Zhang, J.; Mi, X.; Zhang, L.; Luo, S. π-Coordinating Chiral Primary Amine/Palladium Synergistic Catalysis for Asymmetric Allylic Alkylation. *J. Am. Chem. Soc.* **2020**, *142*, 3184−3195. (d) You, C.; Shi, M.; Mi, X.; Luo, S. Asymmetric α-allylic allenylation of β-ketocarbonyls and aldehydes by synergistic Pd/chiral primary amine catalysis. *Nat. Commun.* **2023**, *14*, 2911.

(22) *Ten Chemical Innovations That Will Change Our World: IUPAC identifies emerging technologies in Chemistry with potential to make our planet more sustainable*. https://www.degruyter.com/document/doi/10.1515/ci-2019-0203/html (accessed 2024−02−01).

(23) In the absence of Fe, a significant amount of **1a** remains at the end of the reaction, while **1b** is extensively consumed. A small amount of homocoupling product corresponding to **1b** is observed.

(24) The efficiency of the current reaction initiated by photoredox catalysis can be significantly affected by counterion effects (the NTf_2 counteranion shows superior efficiency compared to others including the OTf counteranion). The degree of ion pairing between the counteranion and the oxidized radical cation intermediate can potentially influence multiple steps in the reaction.

(25) Guingant, A. An Asymmetric Synthesis of (R)-(+)-2-Nonyl-2-(Carbomethoxy) Cyclopentanone, a Known Precursor of the Antibiotic (−)-Malyngolide. *Tetrahedron: Asymmetry* **1991**, *2*, 415−418.

https://doi.org/10.1021/jacs.4c01842
J. Am. Chem. Soc. 2024, 146, 9404−9412

(26) Cossy, J.; Ibhi, S.; Kahn, P. H.; Tacchini, L. A formal synthesis of ptaquilosin the aglycon of a potent bracken carcinogen ptaquiloside. *Tetrahedron Lett.* **1995**, *36*, 7877−7880.
(27) Corrigan, N.; Shanmugam, S.; Xu, J.; Boyer, C. Photocatalysis in organic and polymer synthesis. *Chem. Soc. Rev.* **2016**, *45*, 6165−6212.
(28) Primary radicals can potentially be generated through an alternative process wherein NHP esters are reduced by Fe. The potentials of Fe, photocatalyst, and **1b** were measured in DMF. The results showed that the photocatalyst is capable of reducing Fe(OEP) (II) to Fe (I) ($E_{1/2}$ (Fe (III)/Fe (II)) = −0.42 V vs SCE in DMF; $E_{1/2}$ (Fe (II)/Fe (I)) = −1.23 V vs SCE in DMF; $E_{1/2}$ (Ir (III)/Ir (II)) = −1.21 V vs SCE in DMF). Afterward, Fe(I) can reduce **1b** to form the primary radical species ($E_{1/2}$ (**1b**/**1b**$^{-\bullet}$) = −1.16 V vs SCE in DMF). For details, please see section VIII of the Supporting Information.
(29) Gan, X.-C.; Zhang, B.; Dao, N.; Bi, C.; Pokle, M.; Kan, L.; Collins, M. R.; Tyrol, C. C.; Bolduc, P. N.; Nicastri, M.; Kawamata, Y.; Baran, P. S.; Shenvi, R. Carbon Quaternization of Redox Active Esters and Olefins via Decarboxylative Coupling. *ChemRxiv (Catalysis)* **2023**, DOI: 10.26434/chemrxiv-2023-7vb8x-v2.

https://doi.org/10.1021/jacs.4c01842
J. Am. Chem. Soc. 2024, 146, 9404−9412